

⁶⁸Ga-DOTATOC and FDG PET Imaging of Preclinical Neuroblastoma Models

CLAIRE PROVOST¹, AURÉLIE PRIGNON¹, ALEX CAZES^{2,3}, VALÉRIE COMBARET⁴, OLIVIER DELATTRE^{2,3}, ISABELLE JANOUÉIX-LEROSEY^{2,3}, FRANÇOISE MONTRAVERS^{1,5} and JEAN-NOËL TALBOT^{1,5}

¹Positronic Molecular Imaging Laboratory LIMP, UMS028, Pierre and Marie Curie University, Paris, France;

²Inserm U830, Paris, France;

³Centre for Research, Curie Institute, Paris, France;

⁴Laboratory of Translational Research, Léon Bérard Centre, Lyon, France;

⁵Department of Nuclear Medicine, Tenon Hospital, Paris, France

Abstract. Background/Aim: Somatostatin receptor subtype 2 (SSTR2) are regarded as a potential target in neuroblastoma (NB) for imaging and promising therapeutic approaches. The purpose of this study was to evaluate and compare the SSTR2 status by ⁶⁸Ga-[tetraxetan-D-Phe1, Tyr3]-octreotide (⁶⁸Ga-DOTATOC) positron-emission tomography (PET) and the tumour metabolic activity by ¹⁸F-fluorodeoxyglucose (FDG) PET in different experimental models of NB. Materials and Methods: Three cell lines of human NB with different levels of expression of SSTR2 were grafted into nude mice. Animals were imaged with FDG and ⁶⁸Ga-DOTATOC and the maximum standardized uptake value (SUVmax) was determined to quantify tracer uptake. Ex vivo biodistribution of ⁶⁸Ga-DOTATOC and immunohistochemical analysis of NB xenografts were performed. Results: Compared with FDG, the SUVmax of ⁶⁸Ga-DOTATOC uptake by the tumour was lower but the ratio to background was higher; there was a strong positive correlation between SUVmax values observed with the two tracers ($r^2=0.65$). Sorting the cell lines according to uptake of FDG or ⁶⁸Ga-DOTATOC, injected activity per gram of tissue, Ki67 index or expression of SSTR2 assessed visually led to the same classification. Conclusion: ⁶⁸Ga-DOTATOC allows preclinical imaging of NB according to the intensity of the expression of SSTR2. In contrast with what has been reported for neuroendocrine tumours, in this NB model, the ⁶⁸Ga-

DOTATOC uptake was positively correlated with FDG uptake and with Ki67 index, usual markers of tumour aggressiveness. If confirmed in humans, this result would favour a theranostic application of ⁶⁸Ga-DOTATOC in NB, even in advanced stages.

Neuroblastoma (NB) is the most common extra-cranial solid cancer in human childhood. It arises anywhere along the sympathetic nervous system (1, 2). At present, its diagnosis is difficult. ¹²³Iodine-metaiodobenzylguanidine (¹²³I-MIBG) is currently the reference tracer for single photon-emission computed tomography (SPECT).

Another approach using SPECT imaging for SSTR with the somatostatin analogue ¹¹¹In-pentetreotide has been widely used in neuroendocrine tumours (NET) and also proposed in NB (3). Since 1994, studies have shown that SSTRs are indeed expressed by some NBs (4, 5). Georgantzi *et al.* showed that SSTR2 could be detected by immunohistochemistry in 89% of tumour specimens from 11 children with stage II-IV NB and 78% of experimental tumours derived from five human NB cell lines (6).

SPECT imaging has disadvantages, in particular its limited spatial resolution and sensitivity, and the long duration of image acquisition. PET is becoming the leading functional modality in cancer imaging, as it yields better image resolution, the procedure lasts a shorter time, and a more accurate quantification can be obtained, as compared to SPECT.

At the moment, only a few clinical studies have reported PET imaging in human NB, using metabolic tracers such as the amino acid analogue ¹⁸F-fluorodopa (7) or the glucose analogue FDG (8, 9). Somatostatin analogues designed for PET imaging of SSTR are also available. ⁶⁸Ga-[tetraxetan-D-Phe1, Tyr3]-octreotate (⁶⁸Ga-DOTATATE) and ⁶⁸Ga-DOTATOC are somatostatin analogues suited for PET imaging that display very high SSTR2 receptor binding. ⁶⁸Ga-DOTATATE has been reported for imaging of NB in children and identifying those suitable for molecular

This article is freely accessible online.

Correspondence to: Claire Provost, LIMP Laboratoire d'Imagerie Moléculaire Positronique, Hôpital Tenon 4 rue de la Chine, 75020 Paris, France. Tel: +33 156017298, Fax: +33 156017298, e-mail: claire.provost@upmc.fr

Key Words: PET, neuroblastoma model, somatostatin receptor subtype 2, FDG, ⁶⁸Ga-DOTATOC.

radiotherapy with ^{177}Lu -DOTATATE (10). According to the study of Kroiss *et al.*, ^{68}Ga -DOTATOC may be superior to ^{123}I -MIBG scintigraphy and even to the reference CT/magnetic resonance imaging technique in providing particularly valuable information for pre-therapeutic staging of pheochromocytoma and NB (11).

The use of animal models of NB may be of interest in this context, in order to reduce the number of human studies and be useful for prediction of the efficacy of potential therapeutic regimens. To date, no preclinical studies have dealt with ^{68}Ga -DOTATOC PET in a model of NB, as far as we are aware. The ability of animal tumour models of NB to take up PET tracers has been reported with FDG in spontaneous murine NB (12, 13). Other studies compared FDG with another metabolic tracer 3' [^{18}F]-fluorothymidine in nude mice grafted with NB cell lines (14, 15) or used MIBG labelled with ^{124}I , a PET radionuclide (16).

The purpose of this study was, as first objective, to evaluate the uptake of FDG and ^{68}Ga -DOTATOC using PET imaging in three different animal models of NB, expressing SSTR2 at different levels. A second objective was to study *ex vivo* the biodistribution of ^{68}Ga -DOTATOC in these three NB animal models and correlate this analysis to immunohistochemistry in order to confirm that the tracer uptake was specific for NB.

Materials and Methods

NB cell lines. All cell lines were derived from patients with advanced stages (4s) of disease. CLB-Ga and CLB-Bar NB cell lines were established from tumour specimens obtained from stage 4 bone-marrow metastases and provided by the Léon Bérard Centre (17) and IMR32 was derived from metastatic abdominal site (ATCC LCG, Molsheim, France). Cell lines were maintained in RPMI-1640 with L glutamine (Sigma-Aldrich, St Quentin Fallavier, France) supplemented with 10% foetal calf serum and 1% penicillin/streptomycin (Sigma-Aldrich) at 37°C in a humidified atmosphere containing 5% CO_2 .

SSTR2 expression was measured in these cell lines by quantitative polymerase chain reaction (PCR) using the Power SYBR® Green kit. Total RNA was extracted from NB cell lines using Trizol® and RNA precipitation. Retro-transcription was then performed on 1 µg of RNA with high-capacity cDNA reverse transcription kit (Applied Biosystems, Foster City, CA USA). SSTR2 expression level was calculated relative to the mean expression of CLB-Bar cells and normalized to glyceraldehyde-3-phosphate dehydrogenase (*GAPDH*) expression. The following primers were used: forward 5'-tttgggtgctcctcacctatgct-3'; reverse 5'-tctcattcagccggattgctct-3'.

NB engrafts. Four nude mice (Charles River, l'Arbresle, France) per cell line were subcutaneously grafted in the right flank with 6×10^6 cells/100 µl, re-suspended in PBS and mixed 50/50 with Matrigel (BD Biosciences, Pont de Claix, France). Tumours were measured twice a week with a calliper, the two perpendicular diameters were recorded, and tumour volume (cm^3) was calculated using the formula: $V = \pi/6 \times l \times w^2$, in which l = length and w = width of tumour.

All animal experiments were carried out in compliance with the French laws relating to the conduct of animal experimentation.

^{68}Ga -DOTATOC. DOTATOC was obtained as a lyophilisate (Iason GmbH, Graz-Seiersberg, Austria) and labelled with ^{68}Ga by means of a R&D Synchro module (Raytest, Straubenhardt, Germany). The radiolabelling has already been described elsewhere (18). The overall decay-corrected radiochemical yield was 91 to 94%, radiochemical purity was $\geq 98\%$ using analytical high-performance liquid chromatography and specific radioactivity was 1.95 ± 0.78 MBq/nmol.

PET imaging. PET acquisitions were performed using the Mosaic animal PET machine (Philips Medical systems, Cleveland, OH, USA) on two consecutive days, 6 weeks after grafting, when tumour volume had reached 0.4 to 0.9 cm^3 . Before FDG PET, mice had been fasting for 12 h with free access to water; no fast was applied for the other tracer. Approximately 5 MBq of each PET tracer was injected intravenously in the retro-orbital sinus. PET imaging was started 1 hour after FDG injection or 45 min after ^{68}Ga -DOTATOC injection. Static acquisitions were performed with an exposure time of 10 minutes. Mice were maintained under anaesthesia with 1.5% isoflurane. After acquisition, images were reconstructed and visualised as maximum intensity projection and from different slices (sagittal, transverse, coronal) to allow visual and quantitative analysis, for each animal and each PET tracer. Regions of interest were drawn, surrounding the tumour and a background region corresponding to the soft tissue contralateral to the grafted tumour, using Syntegra-Philips software (PETView; Philips Medical Systems). The uptake was reported as SUVmax, which was calculated as the radioactivity concentration in the ROI (kBq/mL) multiplied by the body weight (g) and divided by the radioactivity injected (kBq). Tumour to background (T/B) SUVmax ratio was also calculated.

Ex vivo biodistribution. One hour after injection of ^{68}Ga -DOTATOC, mice were sacrificed and dissected. The organs and tumours were removed, weighed and the radioactivity counted in a gamma-counter (1480 Wizard 3; Perkin Elmer, Waltham, MA, USA). Tumour and tissue uptake was expressed as the percentage (mean \pm SD) of injected activity per gram of tissue (%ID/g), corrected for ^{68}Ga decay.

Immunohistochemistry. The excised tumours were embedded in paraffin according to standard procedures. The immunostaining of SSTR2 (RBK046-05; Zytomed Systems®, Berlin, Germany) was previously described (18). Haematoxylin-phloxin-safran (HPS) stain was performed for evaluating tissue appearance and proliferation was evaluated by staining of the tumour-proliferating antigen Ki67 in order to assess the tumour aggressiveness. The Ki67 index was calculated as the percentage of positively stained tumour cells among the total number of assessed malignant cells. The tumour slices were observed with an optical microscope in transmitted light (Nikon Eclipse, Champigny sur Marne, France).

Statistical analysis. All data are presented as the mean with standard error of the mean (SEM) or standard deviation (SD). Comparisons were performed using *t*-test for independent or for paired samples, accordingly. The correlation between FDG and ^{68}Ga -DOTATOC uptake was analyzed using Pearson's method to calculate the rank correlation coefficient, *r*. A probability value of less than 0.05 was considered as being statistically significant.

Results

Expression of the SSTR2 gene in NB cell lines. Real-time quantitative PCR showed that the CLB-Ga cells line harboured a low level of SSTR2 expression (0.49 ± 0.82) as compared to CLB-Bar (1.15 ± 0.21 , $p=0.007$) and more strikingly to IMR32 (4.66 ± 0.36 , $p=0.004$), the difference between those two latter cell lines was not significant (Figure 1).

FDG and ^{68}Ga -DOTATOC PET. At the time of imaging, the mean tumour volume, based on calliper measurements, was $0.41 \pm 0.24 \text{ cm}^3$ for CLB-Ga, $0.69 \pm 0.24 \text{ cm}^3$ for CLB-Bar and $0.92 \pm 0.07 \text{ cm}^3$ for IMR32 grafts. These tumour volumes were not statistically different. On PET images, all NB tumours were clearly visualized with both tracers, allowing manual drawing of regions of interest, determination of SUVmax and calculation of the T/B ratio. One example of PET imaging obtained in the same mouse after injection of FDG and then of ^{68}Ga -DOTATOC is displayed in Figure 2.

On FDG PET, the expected biodistribution was observed, with FDG uptake in neck brown fat, in brain and in heart, and elimination of the tracer through the urinary system. Mean (\pm SEM) tumour SUVmax values obtained 1 h after injection of FDG are shown in Figure 3. The SUVmax was the greatest with IMR32 and the lowest with CLB-Ga, the difference being significant ($p=0.008$), without significant differences from CLB-Bar grafted mice Figure 3A. The mean T/B ratio did not differ significantly between CLB-Ga, CLB-Bar and IMR32 grafts (Figure 3B).

^{68}Ga -DOTATOC PET demonstrated rapid tumour uptake in 45 min and rapid clearance from the blood and all tissues, except in organs responsible for elimination (kidneys and bladder). The SUVmax was the greatest with IMR32 and the lowest with CLB-Ga, the difference being significant ($p=0.04$) (Figure 3A). The distribution of T/B ratios followed the same trend as that for SUVmax but no difference was significant (Figure 3B).

SUVmax was greater with FDG than with ^{68}Ga -DOTATOC but the grafts of the three cell lines were better visualised with ^{68}Ga -DOTATOC than with FDG, due to a lower background and better contrast (Figure 3A).

Ex vivo biodistribution of ^{68}Ga -DOTATOC. The biodistribution data are illustrated in Figure 4. Apart from the kidneys, NB tumours had the highest content of radioactivity with the three cell line models. The biodistribution in mice showed excretion of ^{68}Ga -DOTATOC exclusively via the urine. Kidneys had a similar retention in the three models. Other normal organs had a low DOTATOC uptake, below 1%. In the NB tumour, the %ID/g was significantly lower for CLB-Ga grafts ($p=0.03$) vs. IMR32, 1.60 but not significantly different from that of CLB-Bar.

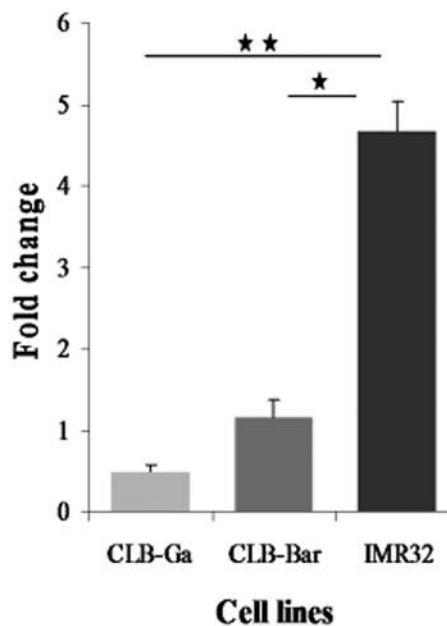


Figure 1. Somatostatin receptor subtype 2 (SSTR2) expression in neuroblastoma cell lines CLB-Ga, CLB-Bar and IMR32 expressed as fold change relative to glyceraldehyde-3-phosphate dehydrogenase. Data are the mean \pm SD. Significantly different at * $p < 0.05$ and ** $p < 0.005$.

Immunohistochemistry. HPS staining confirmed that the tumours corresponded to NB. Ki67 index was 31% for CLB-Ga, 47% for CLB-Bar and 58% for IMR32. Immunohistochemistry with antibody to SSTR2 confirmed the presence of this type of receptor on the three cell lines. The labelling was more intense on the periphery of the cells and was less distinct, or even absent, inside the cells. Visually, the staining was less intense for CLB-Ga than for CLB-Bar grafts and more intense for IMR32 (Figure 5).

Relation between in vivo and ex vivo PET tracer uptake and immunohistochemistry. As expected, there was a significant correlation between the ^{68}Ga -DOTATOC %ID/g of tumour and the SUVmax for ^{68}Ga -DOTATOC in tumour ($r=0.67$, $p=0.03$). Furthermore, the uptake values of FDG and of ^{68}Ga -DOTATOC (expressed as SUVmax) by the NB tumours were positively correlated ($r^2=0.65$, $p=0.005$, Figure 6). Concordantly, sorting the cell lines according to FDG uptake, ^{68}Ga -DOTATOC uptake, Ki67 index or expression of SSTR2 assessed visually led to the same classification with all criteria: CLB-Ga < CLB-bar < IMR32 (Figure 6).

Discussion

NB is a heterogeneous childhood cancer that requires multiple imaging modalities for accurate staging and surveillance. The aim of this preclinical study was to

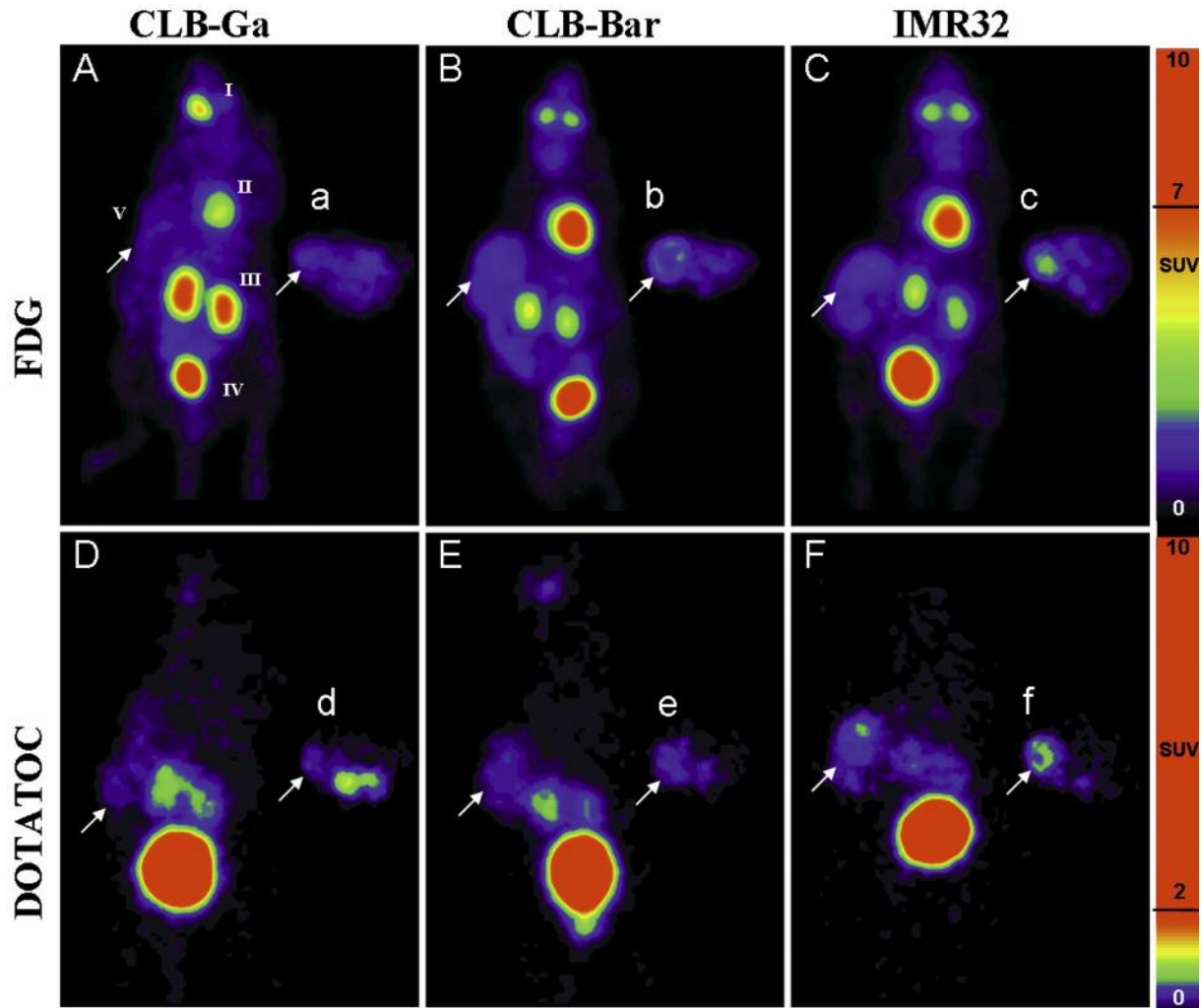


Figure 2. Positron-emission tomography imaging with ^{18}F -fluorodeoxyglucose (FDG) (upper panel) and ^{68}Ga -[tetraacetan-D-Phe1,Tyr3]-octreotide (DOTATOC) (lower panel) in the same mice with xenografts of CLB-Ga, CLB-Bar or IMR32 cell lines. Images are shown in both transaxial (upper case letters) and coronal (lower case letters) slices. Injection site (I), heart (II), kidney (III), bladder (IV), tumour (V). Tumour volume was 0.9 cm^3 for CLB-Ga graft (A, D); 1.2 cm^3 for CLB-Bar graft (B, E) and 1.1 cm^3 for IMR32 graft (C, F).

evaluate and compare the uptake of two tracers for PET imaging, FDG and ^{68}Ga -DOTATOC. We chose PET rather than scintigraphy for the functional molecular imaging of NB since, in humans, PET results in better image resolution and a more accurate quantification of tracer uptake that translates into better diagnostic performance. FDG, the glucose analogue, is the most widely used non-specific metabolic tracer for clinical imaging in oncology. For the detection of human NB lesions, based on their enhanced intracellular glucose transport and metabolism, FDG PET compared favourably with MIBG scintigraphy (19, 20). Even though published evidence is for the moment limited, it has been shown that ^{68}Ga -DOTATOC is also suited to the detection of human NB lesions, based on the overexpression of SSTR

(11); furthermore, this capacity has been well-documented during the past decade for imaging NET. We therefore selected three different nude mouse tumour models of NB, with different *in vitro* expression of SSTR.

Our *in vivo* imaging results, obtained by means of ^{68}Ga -DOTATOC PET, are in accordance with the overexpression of SSTR2 observed on human NB tumours *in vitro*, already described in the literature (4, 5). Our initial assumption that these three types of NB cell lines express SSTR2 at different levels was also confirmed, leading to differential ^{68}Ga -DOTATOC uptake in experimental NB tumours. Both the uptake of ^{68}Ga -DOTATOC and the expression of SSTR2 differed according to tumour type and were the highest for IMR32, intermediary for CLB-bar and the lowest for CLB-

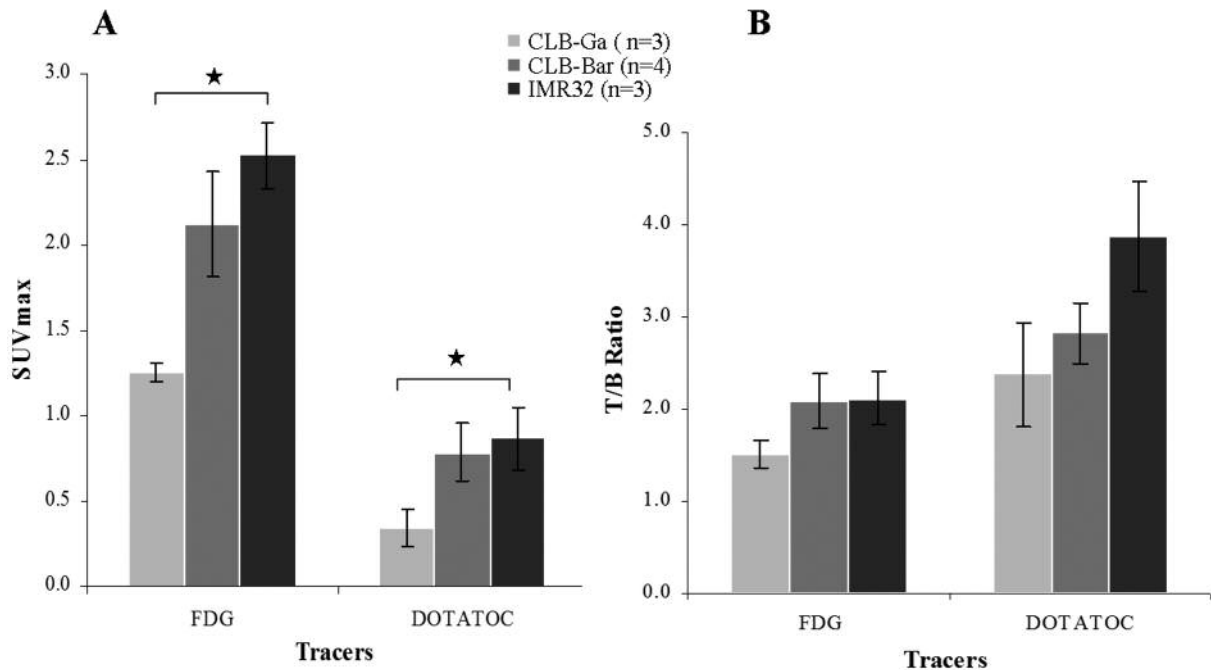


Figure 3. Maximum standardized uptake value (SUVmax) (A) and tumour to background (T/B) ratio (B) for ^{18}F -fluorodeoxyglucose (FDG) and ^{68}Ga -[tetraxetan-D-Phe1,Tyr3]-octreotide (DOTATOC) in three different animal models engrafted with CLB-Ga, CLB-Bar or IMR32 cell lines. Data are the mean \pm standard error of the mean (SEM). *Significantly different at $p < 0.05$.

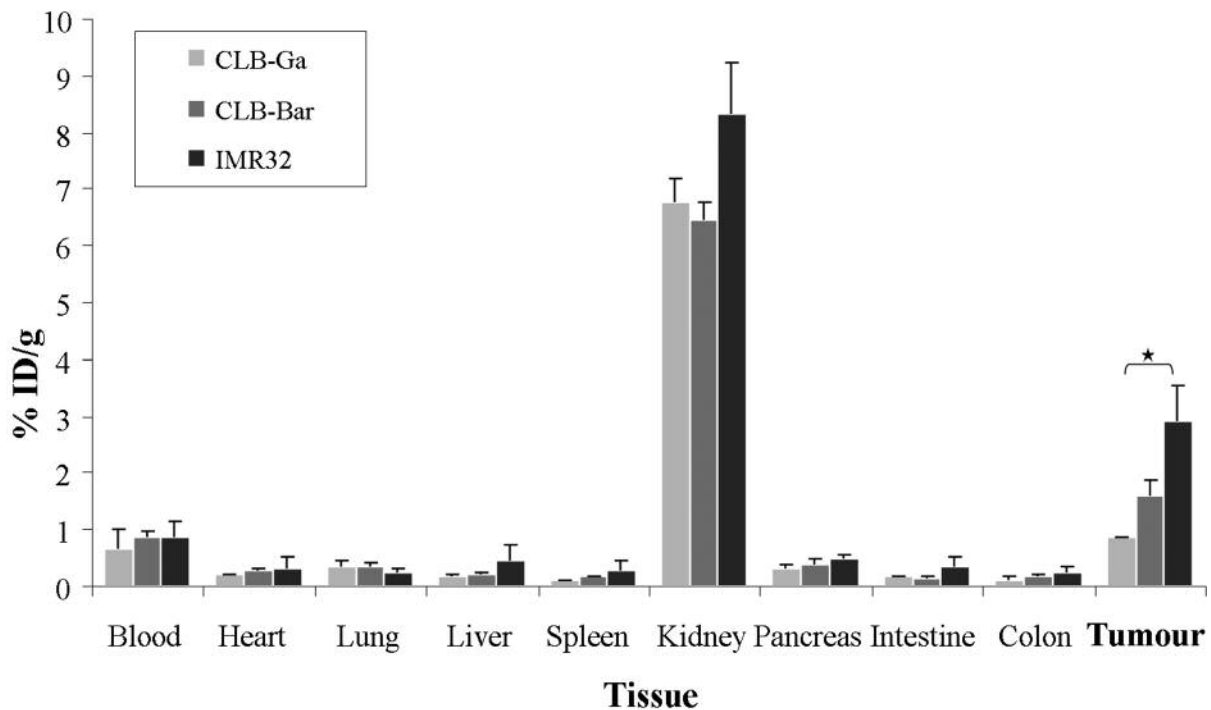


Figure 4. Bar plot of *ex-vivo* ^{68}Ga -[tetraxetan-D-Phe1,Tyr3]-octreotide biodistribution as percentage injected dose per gram (%ID/g) in organs and tumour tissue from three different animal models engrafted with CLB-Ga (n=3), CLB-Bar (n=4) and IMR32 (n=3) cell lines. Data are the mean \pm SEM. *Significantly different at $p < 0.05$.

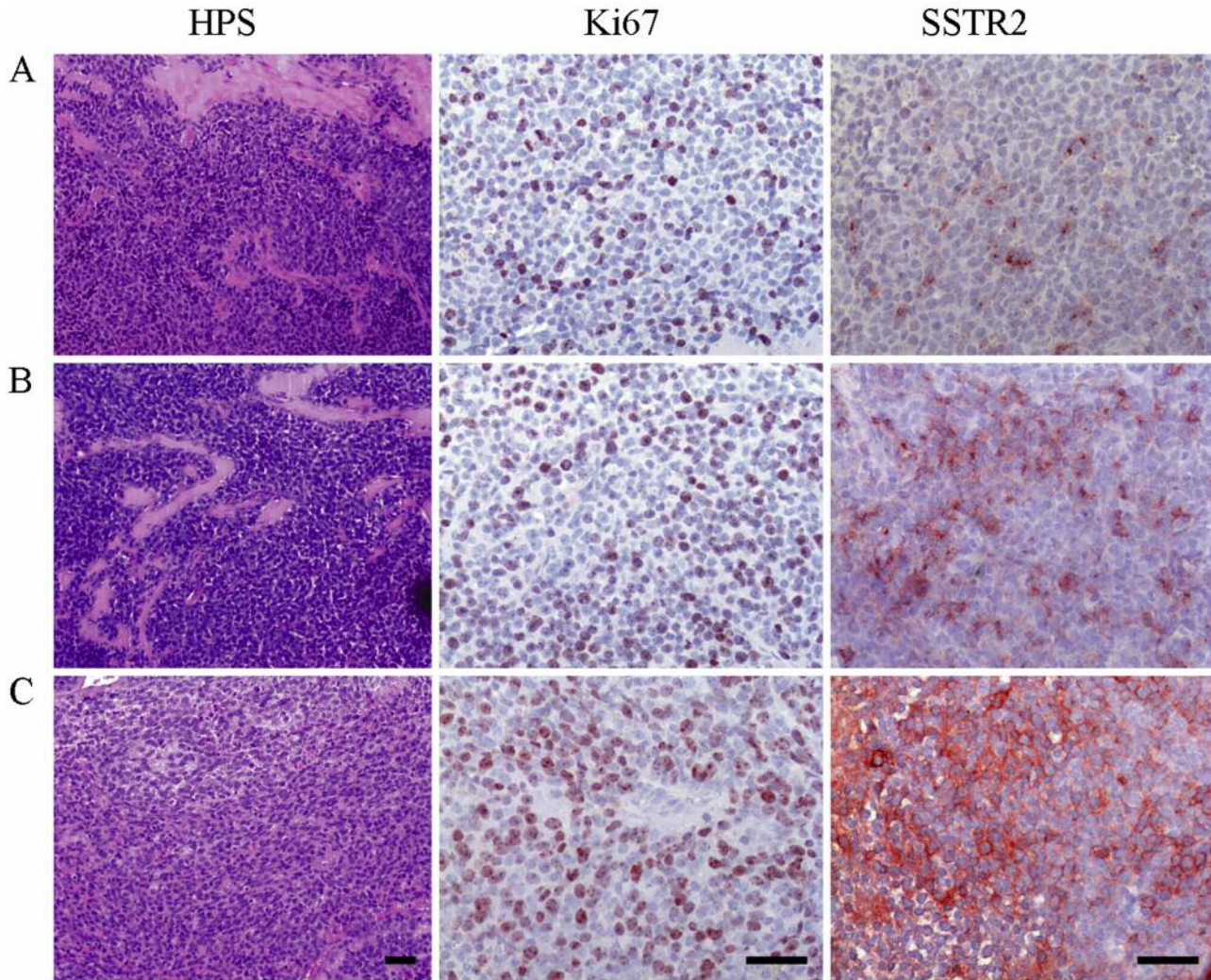


Figure 5. Optical microscopy image for hematoxylin-phloxin-safran (HPS) ($\times 100$), Ki67 ($\times 200$) and antibody to somatostatin receptor subtype 2 (SSTR2) ($\times 200$) on tumours from cell lines CLB-Ga (A), CLB-Bar (B) and IMR32 (C). Scale bar=50 μm .

Ga. This clearly confirms that *in vivo* uptake of ^{68}Ga -DOTATOC, as assessed on PET, is actually linked to the expression of SSTR2 and not to non-specific binding. Concerning the biodistribution of ^{68}Ga -DOTATOC in normal organs of nude mice, our data are consistent with those reported by other teams (21, 22), although the engrafted tumours in their studies were derived from the pancreatic tumour cell line AR4-2J, with low %ID/g in all normal organs except in the kidneys. In humans, ^{68}Ga -DOTATOC PET is significantly taken up in the pancreas, which we and another team did not observe in nude mice (23).

FDG uptake is usually correlated with tumour aggressiveness. In our study, tumour uptake of both tracers appeared to match tumour aggressiveness quantified

through the determination of Ki67. A relation between tumour FDG uptake and Ki67 has been observed in preclinical and in clinical studies for many types of primary cancer, but has not been reported in NB, neither in animal models nor in humans (24). Recently a high FDG uptake ($\text{SUV}_{\text{max}} \geq 3.31$) by NB was demonstrated to be an ultra-high-risk feature that distinguished the most unfavourable genomic types in human NB (8). Surprisingly, in our NB models, the intensity of FDG uptake was also correlated with the expression of SSTR2 and therefore with ^{68}Ga -DOTATOC uptake. This result was not expected since in NET an inverse correlation has been observed: Kayani *et al.* showed a higher uptake of ^{68}Ga -DOTATATE, another somatostatin analogue, in low-

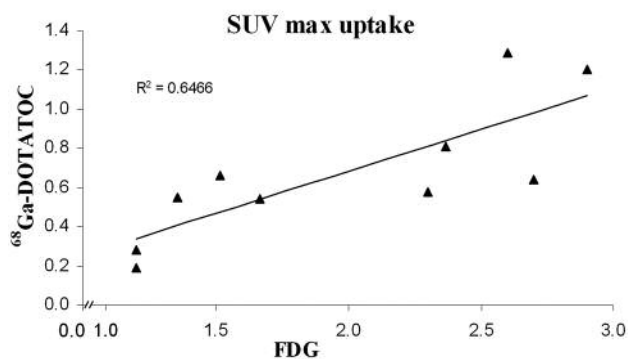


Figure 6. Correlation of maximum standardized uptake value (SUVmax) for ^{18}F -fluorodeoxyglucose (FDG) and ^{68}Ga -[tetraxetan-D-Phe1, Tyr3]-octreotide (^{68}Ga -DOTATOC). Expression of somatostatin receptor subtype 2 (SSTR2) illustrated by ^{68}Ga -DOTATOC uptake correlated positively with FDG uptake value of neuroblastoma tumours with correlation coefficient $R^2=0.65$ and $p=0.005$.

grade NET compared to high-grade NET and, conversely, the FDG uptake was higher in high-grade NET compared with low-grade NET (25). It seems that the pattern of de-differentiation is different in NB and in NET, as our study shows that a high Ki67 is compatible with the overexpression of SSTR, paving the way for the use of 'cold' or radiolabeled somatostatin analogues as an alternative to ^{131}I -MIBG therapy.

Conclusion

For PET imaging of grafted NB tumours that express the SSTR2, FDG had a higher SUVmax than ^{68}Ga -DOTATOC, but tumour visualisation was difficult with FDG because of the high background (blood) and the lack of specificity of the tracer (Figure 3). The contrast from the background and the visualisation of the tumours were significantly better with ^{68}Ga -DOTATOC in engrafts of the IMR32 and CLB-Bar cell lines, with a high expression of SSTR2. Our study confirms that FDG can be useful as a marker of NB cell metabolism, *e.g.* for testing new treatment regimens using PET imaging in murine models of NB. Furthermore, in animal models with spontaneous NB tumour, ^{68}Ga -DOTATOC might be superior for monitoring the effect of a treatment due to its low background and specificity. In contrast with what has been reported in NETs, in NB models used for this study, the ^{68}Ga -DOTATOC uptake was positively correlated with FDG uptake and with Ki67 index, usual markers of tumour aggressiveness. If confirmed in humans, this result would favour a theranostic application of ^{68}Ga -DOTATOC in NB, even in advanced stages.

References

- 1 Brodeur GM, Pritchard J, Berthold F, Carlsen NL, Castel V, Castelberry RP, De Bernardi B, Evans AE, Favrot M and Hedborg F: Revisions of the international criteria for neuroblastoma diagnosis, staging, and response to treatment. *J Clin Oncol* 11: 1466-1477, 1993.
- 2 Castleberry RP: Neuroblastoma. *Eur J Cancer* 33: 1430-1437; discussion 1437-1438, 1997.
- 3 Briganti V, Sestini R, Orlando C, Bernini G, La Cava G, Tamburini A, Raggi CC, Serio M and Maggi M: Imaging of somatostatin receptors by indium-111-pentetreotide correlates with quantitative determination of somatostatin receptor type 2 gene expression in neuroblastoma tumors. *Clin Cancer Res* 3: 2385-2391, 1997.
- 4 Moertel CL, Reubi JC, Scheithauer BS, Schaid DJ and Kvols LK: Expression of somatostatin receptors in childhood neuroblastoma. *Am J Clin Pathol* 102: 752-756, 1994.
- 5 Albers AR, O'Dorisio MS, Balster DA, Caprara M, Gosh P, Chen F, Hoeger C, Rivier J, Wenger GD, O'Dorisio TM and Qualman SJ: Somatostatin receptor gene expression in neuroblastoma. *Regul Pept* 88: 61-73, 2000.
- 6 Georgantzi K, Tsolakis AV, Stridsberg M, Jakobson A, Christofferson R and Janson ET: Differentiated expression of somatostatin receptor subtypes in experimental models and clinical neuroblastoma. *Pediatr Blood Cancer* 56: 584-589, 2011.
- 7 Piccardo A, Lopci E, Conte M, Garaventa A, Foppiani L, Altrinetti V, Nanni C, Bianchi P, Cistaro A, Sorrentino S, Cabria M, Pession A, Puntoni M, Villavecchia G and Fanti S: Comparison of ^{18}F -DOPA PET/CT and ^{123}I -MIBG scintigraphy in stage 3 and 4 neuroblastoma: a pilot study. *Eur J Nucl Med Mol Imaging* 39: 57-71, 2012.
- 8 Liu YL, Lu MY, Chang HH, Lu CC, Lin DT, Jou ST, Yang YL, Lee YL, Huang SF, Jeng YM, Lee H, Miser JS, Lin KH, Liao YF, Hsu WM and Tzen KY: Diagnostic FDG and DOPA positron-emission tomography scans distinguish the genomic type and treatment outcome of neuroblastoma. *Oncotarget* 7: 18774-18786, 2016.
- 9 Papathanasiou ND, Gaze MN, Sullivan K, Aldridge M, Waddington W, Almuhaidib A and Bomanji JB: ^{18}F -FDG PET/CT and ^{123}I -metaiodobenzylguanidine imaging in high-risk neuroblastoma: diagnostic comparison and survival analysis. *J Nucl Med* 52: 519-525, 2011.
- 10 Gains JE, Bomanji JB, Fersht NL, Sullivan T, D'Souza D, Sullivan KP, Aldridge M, Waddington W and Gaze MN: ^{177}Lu -DOTATATE molecular radiotherapy for childhood neuroblastoma. *J Nucl Med* 52: 1041-1047, 2011.
- 11 Kroiss A, Putzer D, Uprimny C, Decristoforo C, Gabriel M, Santner W, Kranewitter C, Warwitz B, Waitz D, Kendl D and Virgolini IJ: Functional imaging in pheochromocytoma and neuroblastoma with ^{68}Ga -DOTA-Tyr 3-octreotide positron emission tomography and ^{123}I -metaiodobenzylguanidine. *Eur J Nucl Med Mol Imaging* 38: 865-873, 2011.
- 12 Cazes A, Lopez-Delisle L, Tsarovina K, Pierre-Eugene C, De Preter K, Peuchmaur M, Nicolas A, Provost C, Louis-Brennetot C, Daveau R, Kumps C, Cascone I, Schleiermacher G, Prignon A, Speleman F, Rohrer H, Delattre O and Janoueix-Lerosey I: Activated ALK triggers prolonged neurogenesis and RET up-regulation providing a therapeutic target in ALK-mutated neuroblastoma. *Oncotarget* 5: 2688-2702, 2014.

- 13 Quarta C, Cantelli E, Nanni C, Ambrosini V, D'Ambrosio D, Di Leo K, Angelucci S, Zagni F, Lodi F, Marengo M, Weiss WA, Pession A, Tonelli R and Fanti S: Molecular imaging of neuroblastoma progression in TH-MYCN transgenic mice. *Mol Imaging Biol* 15: 194-202, 2013.
- 14 Valentiner U, Haane C, Peldschus K, Gustke H, Brenner W, Wilke F, Pommert A, Owsijewitsch M, Schumacher U and Klutmann S: [¹⁸F]FDG and [¹⁸F]FLT PET-CT and MR imaging of human neuroblastomas in a SCID mouse xenograft model. *Anticancer Res* 28: 2561-2568, 2008.
- 15 Krieger-Hinck N, Gustke H, Valentiner U, Mikecz P, Buchert R, Mester J and Schumacher U: Visualisation of neuroblastoma growth in a Scid mouse model using [¹⁸F]FDG and [¹⁸F]FLT-PET. *Anticancer Res* 26: 3467-3472, 2006.
- 16 Seo Y, Gustafson WC, Dannoon SF, Nekritz EA, Lee CL, Murphy ST, VanBrocklin HF, Hernandez-Pampaloni M, Haas-Kogan DA, Weiss WA and Matthay KK: Tumor dosimetry using [¹²⁴I]m-iodobenzylguanidine microPET/CT for [¹³¹I]m-iodobenzylguanidine treatment of neuroblastoma in a murine xenograft model. *Mol Imaging Biol* 14: 735-742, 2012.
- 17 Schleiermacher G, Raynal V, Janoueix-Lerosey I, Combaret V, Aurias A and Delattre O: Variety and complexity of chromosome 17 translocations in neuroblastoma. *Genes Chromosomes Cancer* 39: 143-150, 2004.
- 18 Chereau E, Durand L, Frati A, Prignon A, Talbot JN and Rouzier R: Correlation of immunohistopathological expression of somatostatin receptor-2 in breast cancer and tumor detection with ⁶⁸Ga-DOTATOC and ¹⁸F-FDG PET imaging in an animal model. *Anticancer Res* 33: 3015-3019, 2013.
- 19 Bleeker G, Tytgat GA, Adam JA, Caron HN, Kremer LC, Hooft L and van Dalen EC: ¹²³I-MIBG scintigraphy and ¹⁸F-FDG-PET imaging for diagnosing neuroblastoma. *Cochrane Database Syst Rev* 9: CD009263, 2015.
- 20 Dhull VS, Sharma P, Patel C, Kundu P, Agarwala S, Bakshsi S, Bhatnagar V, Bal C and Kumar R: Diagnostic value of ¹⁸F-FDG PET/CT in paediatric neuroblastoma: comparison with ¹³¹I-MIBG scintigraphy. *Nucl Med Commun* 36: 1007-1013, 2015.
- 21 Ugur O, Kothari PJ, Finn RD, Zanzonico P, Ruan S, Guenther I, Maecke HR and Larson SM: Ga-66 labeled somatostatin analogue DOTA-DPhe1-Tyr3-octreotide as a potential agent for positron emission tomography imaging and receptor mediated internal radiotherapy of somatostatin receptor positive tumors. *Nucl Med Biol* 29: 147-157, 2002.
- 22 Stelter L, Amthauer H, Rexin A, Pinkernelle J, Schulz P, Michel R, Denecke T, Stiepani H, Hamm B, Wiedenmann B and Scholz A: An orthotopic model of pancreatic somatostatin receptor (SSTR)-positive tumors allows bimodal imaging studies using 3T MRI and animal PET-based molecular imaging of SSTR expression. *Neuroendocrinology* 87: 233-242, 2008.
- 23 Zhang H, Moroz MA, Serganova I, Ku T, Huang R, Vider J, Maecke HR, Larson SM, Blasberg R and Smith-Jones PM: Imaging expression of the human somatostatin receptor subtype-2 reporter gene with ⁶⁸Ga-DOTATOC. *J Nucl Med* 52: 123-131, 2011.
- 24 Ito M, Shien T, Kaji M, Mizoo T, Iwamoto T, Nogami T, Motoki T, Taira N, Doihara H and Miyoshi S: Correlation between ¹⁸F-fluorodeoxyglucose positron emission tomography/computed tomography and clinicopathological features in invasive ductal carcinoma of the breast. *Acta Med Okayama* 69: 333-338, 2015.
- 25 Kayani I, Bomanji JB, Groves A, Conway G, Gacinovic S, Win T, Dickson J, Caplin M and Ell PJ: Functional imaging of neuroendocrine tumors with combined PET/CT using ⁶⁸Ga-DOTATATE (DOTA-DPhe1,Tyr3-octreotate) and ¹⁸F-FDG. *Cancer* 112: 2447-2455, 2008.

Received July 7, 2016

Revised July 29, 2016

Accepted August 1, 2016